VII. CONCLUSIONS

In this work SiC was grown on Si and 6H-SiC substrates by CVD method. 3C-SiC was grown by a combination of carbonization and CVD growth on Si substrates. The following conclusions concerning crystal growth of 3C-SiC were obtained.

1) In RHEED observation carbonized layers on Si(100) showed a spot pattern of single crystalline 3C-SiC. However, extra spots and streaks due to crystal defects were observed, which were probably due to lattice mismatch between Si and 3C-SiC. The grown layer showed an improvement of crystallinity due to increase of the film thickness in a few characterization methods.

2) Cubic SiC was grown on Si(100), (111), (110) and (211) faces. Single crystals were obtained on (100) and (111) substrates. However, single crystal growth of SiC nonpolar surfaces such as (110) and (211) was unsuccessful, which was considered to be due to the formation of the first grown C layer by carbonization in spite that the layer should consist of both C and Si atoms.

3) The layers grown on Si(100) well oriented substrates contained antiphase domains. The origin of the antiphase domains was considered to have the close relationship with the surface step height. Growth on spherically polished (100) substrates was carried out, and introduction of off orientation towards (011) was found to be effective for elimination of antiphase domains. Antiphase-domains free layers grown on Si(100) off substrates showed electrical anisotropy.

About impurity doping and device fabrication of 3C-SiC on Si the following conclusions were obtained.

4) To obtain p-type conduction B and Al were doped during growth using B_2H_6 and organic Al, respectively. The B-doped layer showed high resistive p-type conduction. The maximum resistivity obtained was $8\times10^3\Omega$cm. By Al-doping the hole concentration was controlled in the range of 3×10^{16}-2×10^{17}cm^{-3}. A typical hole mobility in the Al-doped layer was 30cm^2/Vs. Too much doping by

both dopants resulted in rough surfaces. Organic Al worked as a dopant and a carbon source simultaneously.

5)Ion implantation of donors of P^+ and N_2^+ was carried out into the p-type layers. The annealing temperature dependence of electrical characteristics was investigated. Electrical activation increased monotonously as annealing temperature became higher. N_2^+ implanted layers showed larger electrical activation than P^+ implanted layers. Capacitance-voltage characteristics of the p-n junction diodes fabricated using ion implantation technique showed that the diodes had a p-i-n structure.

6)Inversion-type MOSFET's of cubic SiC were fabricated. Antiphase-domains free layers grown on Si(100) off substrates were used. A gate oxide of SiO_2 was formed by thermal oxidation. Source and drain were formed by ion implantation of P^+ into the B-doped p-layer. Inversion mode operation was confirmed for the first time. Current-voltage characteristics of the FET's showed a tendency of saturation.

By the investigation of growth on 6H-SiC, the following conclusions were obtained.

7) Crystals of SiC were grown on 6H-SiC(0001)Si faces at 1350-1500°C by CVD method. In this temperature region, 3C-SiC twin crystals were grown on a natural face. However, 6H-SiC was grown at 1400-1500°C by the introduction of off orientation into substrates. This temperature is 300-400°C lower than ordinary growth temperatures of around 1800°C. The change in polytypes by off orientation of substrates was explained in relation to the surface step density. At 1350°C twin crystals of 3C-SiC were grown both on natural faces and off substrates.

8) P-n junction diodes of 6H-SiC were fabricated at 1500°C by CVD growth. The diodes showed good rectification. A breakdown electric field of 2.4×10^6V/cm was achieved in the junction. This fact indicates that the crystallinity of 6H-SiC grown at low temperatures is comparable to that grown at high temperatures. The diodes showed blue-light emission in the forward bias region.

Finally for further investigation some suggestions are given

as follows. Layers grown on Si are considered to remain a problem of lattice mismatch. To solve the problems an innovation is necessary for the growth method. One considerable way is to utilize the grown layer as a substrate for the next growth. For the second growth method, sublimation, LPE and CVD at higher temperatures are hopeful. By sublimation method high growth rate and growth of ingots are expected. Very thick grown layers may not inherit the influence of lattice mismatch. LPE growth at equilibrium may have a possibility of the improvement of crystallinity. CVD growth at temperatures over the melting point of Si will give rise to variation in the mechanism of crystal growth, which was observed for the growth on 6H-SiC. Preliminary trials of some of these methods are already started[1,2].

Excellent results were obtained as a preliminary trial concerning homoepitaxial growth of 6H-SiC in this work. However, easily obtainable substrates are still far from satisfactory. Uniformity in shapes, sizes, impurities and crystallinity should be improved for a systematic investigation.

Reproducibility in electrical properties is not good under the present technique. Undoped carrier concentration sometimes changes unintentionally. For device application an improvement of this point is necessary. To raise the level of CVD growth technique, every part used around the gas system and the reaction tube should be reconsidered whether their qualities are adequate or not. Especially, since a susceptor, its quartz holder and a quartz reaction tube are heated during growth, they are likely to supply impurities. Their materials and how to handle them should be important problems.

References

[1] W.S.Yoo, S.Nishino and H.Matsunami, Mem. Fac. Eng. Kyoto Univ., 49(1987) 21.

[2] T.Takeuchi, private communication.

LIST OF PUBLICATION

I.Papers and Letters

(1) "Metal-Oxide-Semiconductor Characteristics of Chemical Vapor Deposited Cubic-SiC"
by K.Shibahara, S.Nishino and H.Matsunami
in Jpn. J. Appl. Phys. Part 2, vol.23(1984) pp.L862-L864.

(2) "Plasma Etching of CVD Grown Cubic SiC Single Crystals"
by S.Dohmae, K.Shibahara, S.Nishino and H.Matsunami
in Jpn. J. Appl. Phys. Part 2, vol.24(1985) pp.L873-L875.

(3) "SURFACE MORPHOLOGY OF CUBIC SiC(100) GROWN ON Si(100) BY CHEMICAL VAPOR DEPOSITION"
by K.Shibahara, S.Nishino and H.Matsunami
in J. Crystal Growth, vol.78(1986) pp.538-544.

(4) "Fabrication of Inversion-Type n-Channel MOSFET's Using Cubic-SiC on Si(100)"
by K.Shibahara, T.Saito, S.Nishino and H.Matsunami
in IEEE Electron Device Letters, vol.EDL-7(1986) pp.692-693.

(5) "Heteroepitaxial Growth of SiC on Si substrates"
by K.Shibahara, S.Nishino and H.Matsunami
in J. Jpn. Association of Crystal Growth, vol.13(1986) pp.226-232, in Japanese.

(6) "Antiphase-domain-free growth of cubic SiC on Si(100)"
by K.Shibahara, S.Nishino and H.Matsunami
in Appl. Phys. Lett. vol.50(1987) pp.1888-1890.

(7) "Fabrication of P-N Junction Diodes Using Homoepitaxially Grown 6H-SiC at Low Temperature by Chemical Vapor Deposition"
by K.Shibahara, N.Kuroda, S.Nishino and H.Matsunami
in Jpn. J. Appl. Phys. Part 2 vol.26(1987) pp.L1815-L1817.

(8) "Reflection high energy electron diffraction observation of cubic SiC on Si(100) grown by chemical vapor deposition"
by K.Shibahara, S.Nishino and H.Matsunami
To be submitted to J. Appl. Phys.

(9) "POLYTYPE CONTROL OF CVD GROWN SiC ON 6H-SiC SUBSTRATES"
by K.Shibahara, N.Kuroda, S.Nishino and H.Matsunami
To be submitted to J. Crystal Growth.

(10) "Electrical Properties of Undoped and Ion Implanted Cubic SiC Grown on Si by Chemical Vapor Deposition"
by K.Shibahara, T.Takeuchi, S.Nishino and H.matsunami
To be submitted to Jpn. J. Appl. Phys.

(11) "CVD Growth of Cubic SiC on Spherically Polished Si(111) Substrates"
by K.Shibahara, N.Kuroda, S.Nishino and H.Matsunami
To be submitted to Jpn. J. Appl. Phys. Short Note.

II.Proceedings of Conferences

(1) "Production of Single Crystalline Cubic-SiC with 2-inch Diameter by CVD and Characteristics of MOS Diodes"
by S.Nishino, K.Shibahara, S.Dohmae and H.Matsunami
in Late News Abstract of 16th 1984 International Conference on Solid State Devices and Materials, Tokyo, pp.8-9.

(2) "Inversion-type N-Channel MOSFET Using Antiphase-domain Free Cubic-SiC Grown on Si(100)"
by K.Shibahara, T.Saito, S.Nishino and H.Matsunami
in Extended Abstract of 18th 1986 International Conference on Solid State Devices and Materials, Tokyo, pp.717-718.

(3) "HETEROEPITAXIAL GROWTH OF ANTIPHASE-BOUNDARY FREE CUBIC SIC(100) SINGLE CRYSTALS ON SI(100)"
by K.Shibahara, S.Nishino and H.Matsunami

in Material Society Symposia Proceedings vol.97(1987), Anaheim, USA, pp.183-188.

(4) "INVERSION-TYPE MOS FIELD EFFECT TRANSISTORS USING CVD GROWN CUBIC SIC ON SI"
by K.Shibahara, T.Takeuchi, T.Saitoh, S.Nishino and H.Matsunami
in Material Society Symposia Proceedings vol.97(1987), Anaheim, USA, pp.247-252.

(5) "Step-Controlled VPE Growth of SiC Single Crystals at Low Temperatures"
by N.Kuroda, K.Shibahara, W.Yoo, S.Nishino and H.Matsunami
in Extended Abstract of 19th Conference on Solid State Devices and Materials, Tokyo, 1987, pp.227-230.

APPENDIX: Electron diffraction patterns

In order to obtain theoretical patterns of electron diffraction, three factors such as the reciprocal lattice, structure factor and double diffraction should be taken into account. They are explained in order below.

All polytypes of SiC can be treated using hexagonal-type primitive cells. Usually Millar-Bravais indices such as $(hkil)$ and $(hk{\cdot}l)$*) are used to identify lattice planes of SiC, because this notation explicitly expresses symmetrical relationships between various faces in a hexagonal lattice. However, this notation is not benefit for vector calculation. Therefore, concerning diffraction Miller indices such as (hkl) are mainly used in this thesis. Though Miller indices for a cubic lattice are more popular for 3C-SiC, here all polytypes are treated as hexagonal lattices to keep generality of discussion. Readers should take care to avoid confusion due to interminglement of these notations.

*) Here, i must be equal to $-(h+k)$[1]. Therefore, i can be omitted and substituted by a dot. It must be remembered that $(hk{\cdot}l)$ is equal to $(hkil)$ and not equal to (hkl).

(i) Reciprocal lattice of SiC

A primitive cell of SiC is defined by primitive vectors of a_1, a_2 and a_3 shown in Fig.1. SiC consists of repetition of tetrahedrons shown in Fig.2. The length of edges of the tetrahedron is equal to $|a_1|$ and $|a_2|$ and its height is equal to $|a_3|/n$. Therefore, $|a_1|=|a_2|=|a_3|/(n\sqrt{6}/3)=a_0=3.08\text{Å}$. n is a number of layers in the repeat distance of a primitive cell in the [001] direction. The <001> direction is a so-called c-axis direction. a_1, a_2 and a_3 are expressed as follows:

$$a_1 = a_0\begin{pmatrix}\cos 30°\\ \sin 30°\\ 0\end{pmatrix}, \quad a_2 = a_0\begin{pmatrix}\cos 150°\\ \sin 150°\\ 0\end{pmatrix}, \quad a_3 = a_0\begin{pmatrix}0\\ 0\\ n\sqrt{6}/3\end{pmatrix}. \qquad (1)$$

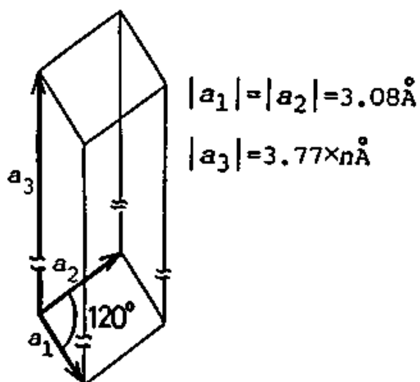

Fig.1 Primitive cell of SiC.

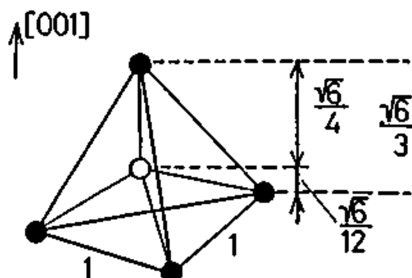

Fig.2 Tetrahedron component of SiC crystals.

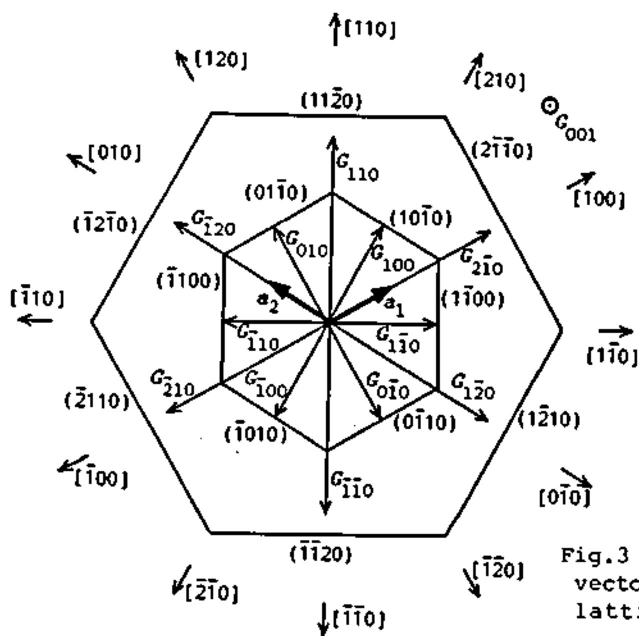

Fig.3 Orientations of reciprocal vectors, lattice directions and lattice planes.

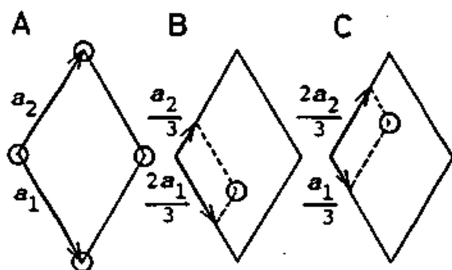

Fig.4 Positions of atoms in *A*-, *B*- and *C*-layers.

The axis vectors b_1, b_2 and b_3 of the reciprocal lattice are given as follows[2]:

$$b_1 = (2\pi/V)a_2 \times a_3 \ ,$$
$$b_2 = (2\pi/V)a_3 \times a_1 \ , \qquad (2)$$
$$b_3 = (2\pi/V)a_1 \times a_2 \ ,$$

where $V = a_1 \cdot a_2 \times a_3$.

Therefore, the axis vectors of the reciprocal lattice for SiC are obtained as follows:

$$b_1 = b_0 \begin{pmatrix} \cos 60° \\ \sin 60° \\ 0 \end{pmatrix}, \ b_2 = b_0 \begin{pmatrix} \cos 120° \\ \sin 120° \\ 0 \end{pmatrix}, \ b_3 = b_0 \begin{pmatrix} 0 \\ 0 \\ 3\sqrt{2}/4n \end{pmatrix}, \qquad (3)$$

where $b_0 = (4\pi\sqrt{3}/3)a_0)$.

In the real space the angle between a_1 and a_2 was 120°, however, in the reciprocal space the angle between b_1 and b_2 is 60°. A reciprocal lattice vector G_{hkl} is defined as follows:

$$G_{hkl} = hb_1 + kb_2 + lb_3 \quad (h,k,l\text{: integers}) . \qquad (4)$$

G_{hkl} is perpendicular to (hkl) and $2\pi/|G_{hkl}|$ is equal to lattice spacing of (hkl). Figure 3 shows relatioships concerning orientations among the reciprocal lattice vectors, lattice directions expressed by Mirror indices and lattice planes expressed by Mirror-Bravais indices. (hkl) is perpendicular to $G_{h\underline{k}\underline{l}}$ and omitted in Fig.3. (hkl) is not perpendicular to $[hkl]$. $\{2\bar{1}\bar{1}0\}$ and $\{10\bar{1}0\}$ planes are drawn by a large and small hexagons, respectively. In the case of Mirror-Bravais indices $\{2\bar{1}\bar{1}0\}$ and $\{10\bar{1}0\}$ planes are perpendicular to $\langle 2\bar{1}\bar{1}0 \rangle$ and $\langle 10\bar{1}0 \rangle$ directions.

(ii) Structural factor

The condition of diffraction is given as follows using the wave vector k of an incident beam($|k| = 2\pi/\lambda$, λ: wave length of the incident beam)[2]:

$$2k \cdot G_{hkl} = G^2 \ , \qquad (5)$$

where G is $|G_{hkl}|$. However, even if G_{hkl} satisfies this equation, sometimes diffraction cannot be observed. For example, diffraction due to Si(100) and (200) is not observed in the case of X-ray diffraction. Such phenomena are explained by the

structure factor. The structure factor S is given as [2]

$$S(G_{hkl})=\sum_j f_j \exp(-2\pi i(hx_j+ky_j+lz_j)) , \quad (6)$$

$$r_j= x_j a_1 + y_j a_2 + z_j a_3 , \quad (7)$$

where r_j is the vector to the center of atom j in a primitive cell and f_j atomic form factor. The atomic form factor is common to the atoms of a kind. Scattering intensity is proportional to $S \cdot S^*$. When $S=0$, diffraction is not observed.

The structure factor of SiC is obtained by the procedure explained below. Structures of all polytypes of SiC are identified by stacking sequences of layers in <001> direction as explained in Chapter I. For example, 3C and 6H-SiC have the staking sequences of ABC and $ABCACB$. The primitive cell of SiC contains n Si atoms and n C atoms. The positions of atoms in the primitive cell are expressed utilizing the stacking sequence. Locations of atoms in each layer are shown in Figs.4(a)-(c). Each Si atom locates $|a_3/4n|$ away from the nearest C atom belonging to the same layer as shown in Fig.2. When a Si atom locates at the origin and belong to A-layer the structure factor S is given for all polytypes as follows:

$$S= (f_{Si}+\exp(-2\pi i/4n)f_C)\cdot \sum_{j=0}^{n-1} \exp(-2\pi i(g_j+il/n)) , \quad (8)$$

$$g_j(\text{A-layer})=0, \ g_j(\text{B-layer})=(-h+k)/3, \ g_j(\text{C-layer})=(h-k)/3 , \quad (9)$$

Where f_{Si} and f_C are the atomic form factors for Si and C. $(f_{Si}+\exp(-2\pi i/4n)f_C)$ will not be zero for any G_{hkl} and the next formula can be used to obtain G_{hkl} which makes S be zero.

$$S'=\sum_{j=0}^{n-1} \exp(-2\pi i(g_j+il/n)) , \quad (10)$$

For example S' of 2H-SiC whose stacking order is AB is explicitly expressed as follows:

$$S'_{2H}=1+\exp(-2\pi i(-h+k)/3)\cdot\exp(-\pi il) . \quad (11)$$

If l is an odd number and $(-h+k)$ is a multiple of 3, S' and S will be zero.

(iii) Prediction of diffraction pattern

When G_{hkl} satisfies eq.(5) and $S'(G_{hkl})\neq 0$, diffraction is observed as a spot on a screen. In order to obtain reciprocal vectors which satisfy eq.(5), the construction due to Ewald[3] is convenient. So-called the Ewald sphere of $|k|$ in a radius which contact with the origin of reciprocal space is drawn. Reciprocal lattice points which contact with the Ewald sphere give rise to diffraction. In the case of electron diffraction, a radius of the Ewald sphere is much larger than the axis vectors of the reciprocal lattice. Therefore, nearby the origin, the Ewald sphere is approximated by a plane normal to the incident beam. The reciprocal points which contact with the plane are given using two reciprocal vectors which are not parallel to each other and perpendicular to the incident beam. A map of these reciprocal points appears as diffraction pattern on a screen.

In the case of RHEED observation of SiC(0001), G_{001} is always perpendicular to the incident azimuth. Another vector which is perpendicular to the incident azimuth is achieved by referring Fig.3. For examples, G_{010} and $G_{1\bar{2}0}$ are perpendicular to [100] and [210] azimuths, respectively. A [100] azimuth RHEED pattern of 2H-SiC(0001) is drawn as follows. G_{010} and G_{001} are perpendicular to [100] azimuth. Grid points given by $m_1G_{010}+m_2G_{001}$ (m_1, m_2: integer) represent a observable pattern. These two vectors are perpendicular to each other and $|G_{010}|/|G_{001}|=1.89$ based on eqs.(3) and (4)*). Therefore, the pattern is drawn and indices are given to each point as shown in Fig.5. In the case of RHEED observation, spots given by negative values of m_2 cannot be observed shaded by a specimen. A spot due to G_{hkl} which makes $S'(G_{hkl})$ zero is drawn by an white circle and others are drawn by solid circles. However, spots indicated by white circles are actually observed because of the double diffraction[4]. If diffraction due to $G_{h1,k1,l1}$ and $G_{h2,k2,l2}$ takes place, diffraction due to $G_{h1\pm h2,k1\pm k2,l1\pm l2}$ also takes place even if $S(G_{h1\pm h2,k1\pm k2,l1\pm l2})$ is equal to zero. Such a phenomena is called the double diffraction. For example, G_{001} in

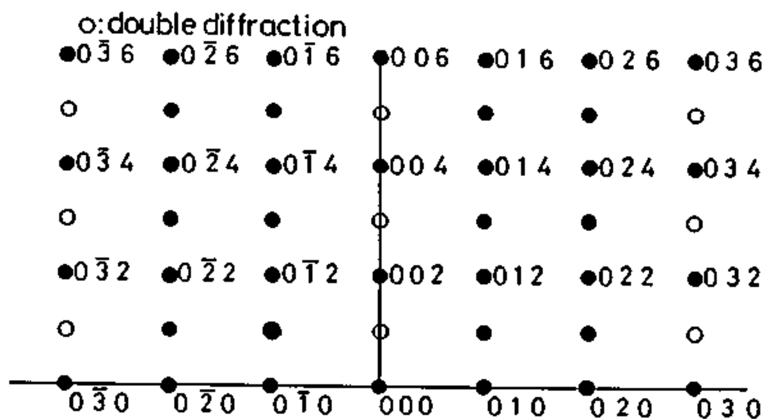

Fig.5 [100](or [2$\bar{1}\bar{1}$0]) azimuth RHEED pattern of 2H-SiC(0001).

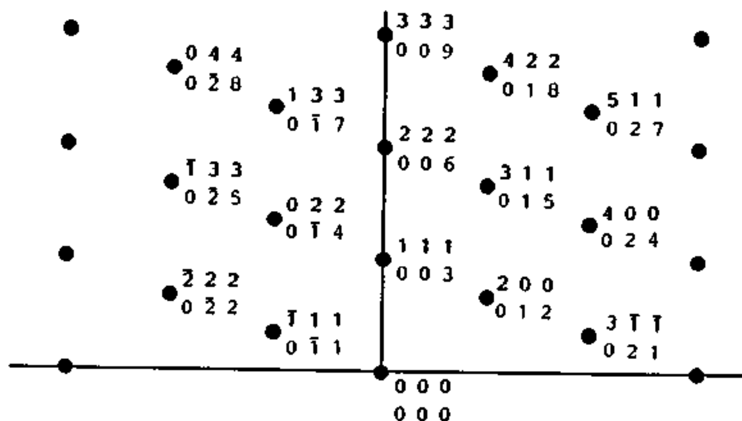

Fig.6 [100] azimuth pattern of 3C-SiC(0001). This expression is equal to "[01$\bar{1}$] azimuth pattern of 3C-SiC(111)" for cubic notation. Indicies for hexagonal and cubic notations are written in normal and bold-faced characters.

Fig.5 is synthesized by G_{100} and G_{101}.

In the discussion above, all polytypes of SiC are treated as hexagonal lattices. However, symetrical relationships peculiar to 3C-type cannot be explicitly expressed by this way. For comparison of notations for a hexagonal and a cubic lattice, A [100] azimuth pattern of 3C-SiC(0001) (or a $[01\bar{1}]$ azimuth pattern of 3C-SiC(111) in cubic notation) is shown in Fig.6. Indices are given by the both notations.

*) The lattice spacing d_{hkl} of (hkl) faces in hexagonal lattice is given by following expression.

$$d_{hkl}^{-2}=(4/3)(h^2+hk+k^2)/a+l^2/c^2 \quad (a=|a_1|=|a_2|,\ c=|a_3|)\ .$$

$|G_{hkl}|$ is also calculated utilizing this formula.

References

[1] B.D.Cullity, *Elements of X-ray Diffraction*, (Addison-Wesley, Massachusetts, 1956) Chapter 2.

[2] C.Kittel, *Introduction to Solid State Physics*, (Wiley, New York, 1986) 6th ed., Chapter 2.

[3] M.Plutton, *Surface Physics*, (Oxford Univ. Press, Oxford, 1975), Chapter 3.

[4] P.B.Hirsch, A.Howie, R.B.Nicholson, D.W.Pashley and M.J.Whelan, Electron Microscopy of Thin Crystals, (Butterworths, London, 1965), Chapter 6.